# The effect of creep damage formulation on crack tip fields, creep stress intensity factor and crack growth assessments

V. Shlyannikov
*Kazan Scientific Center of the Russian Academy of Sciences, Russia*
*shlyannikov@mail.ru, http://orcid.org/0000-0001-2345-6789*

A. Tumanov
*Kazan Scientific Center of the Russian Academy of Sciences, Russia*
*tumanoff@rambler.ru, http://orcid.org/0000-0002-2345-6790*

**ABSTRACT.** Fields of stress, strain rate and process zone of a mode I creep crack growth are analyzed by employing damage evolution equations. Damage models for fracture of process zone represented by stress based formulation. Two expressions are presented to describe the stress-sensitive nature of multi-axial rupture behavior. Both damage free and defective creeping solids have been studied. The variation of creep stress and the crack-tip governing parameter in the form of creep $I_n$-integral with time and the evolution of creep damage were analyzed by using the FE-model. The effect of the introduced creep stress intensity factor as a function of creep time through the continuum damage mechanics of the creep crack growth are discussed in detail.

**KEYWORDS.** Creep damage; Creep SIF; Multi-axial stress function.



**Citation:** Shlyannikov, V., Tumanov, A., The effect of creep damage formulation on crack tip fields, creep stress intensity factor and crack growth assessments, Frattura ed Integrità Strutturale, 41 (2017) 285-292.

**Received:** 28.02.2017
**Accepted:** 03.05.2017
**Published:** 01.07.2017



## INTRODUCTION

The high temperature damage accumulation and growth that occurs under creep conditions unites of changes in material microstructure, void nucleation, interaction and growth on grain boundaries leading to creep rupture. A number of approaches have been proposed in the literature for the damage analysis and the estimation of stress-strain rate variation at the crack tip in creeping solids [1-8]. Some of them take into account the effect of multi-axial states of stress in the form of stress and ductility based models [1,2,8]. The authors analyzed the influence of creep damage on crack tip fields under small-scale and extensive creep conditions by the use of an asymptotic analyses [5,6] and finite element method [7].

In this paper, attention is directed on defective solids behavior in which stress-strain state changed as a result of the damage accumulation at the crack tip for steady state secondary creep conditions. The multi-axial stress function and continuum damage model are discussed and developed in order to assess the creep crack growth on the basis of a creep stress intensity factor.

## MULTI-AXIAL RUPTURE BEHAVIOR

The many experimental results of uniaxial tension creep rupture tests of structural materials different properties show that the stress rupture time behavior can be accurately described by power-law equation

$$t = A\sigma^{-\delta} \tag{1}$$

where $A$ and $\delta$ are constants independent of stress for a given material. Values of $\delta$ for a variety of materials tested at different temperatures described by an approximate relationship with the Norton equation exponent $\delta = 0.7n$. It has been shown by Hayhurst [1] that under multi-axial loading conditions the constant $A$ should be a function of the stress invariants

$$t = A\left\{\alpha\sigma_{mp} + \beta J_1 + \gamma\sqrt{J_2'}\right\}^{-\delta} \tag{2}$$

where $\sigma_{mp}$ is the maximum principal tensile stress, $J_1$ is the first stress invariant, $J_2'$ is the second deviatoric stress invariant, $\alpha, \beta$ and $\gamma$ are constants $(\alpha + \beta + \gamma = 1)$. In terms of principal stresses $J_1$ and $J_2'$ are given by

$$J_1 = \sigma_1 + \sigma_2 + \sigma_3, \quad J_2' = \frac{1}{6}\left[(\sigma_1 + \sigma_2)^2 + (\sigma_2 + \sigma_3)^2 + (\sigma_3 + \sigma_1)^2\right] \tag{3}$$

The most general multi-axial creep rupture criterion is obtained by Pisarenko-Lebedev [2], which unites the limiting state theories in the form of the maximum principal tensile stress and the von Mises condition

$$\sigma_{eff} = (1-\chi)\sigma_{mp} + \chi\sqrt{J_2'} \tag{4}$$

in which $\chi$ is the experimental material constant that is determined as the ratio of uniaxial tensile to compression strength $\chi=\sigma_t/\sigma_c$. For brittle fracture $\chi=0$, while for ductile fracture $\chi=1$. Hayhurst [1] have mentioned that a general representation of multi-axial creep rupture behavior must exhibit the sensitivity of micro-structural changes to the maximum principal tensile stress and express the stress sensitivity of different materials to final collapse or failure mechanism. The preceding review of creep rupture equations indicates that a general formulation of stress function which satisfies these requirements can be consists two parts:

- in the tension-tension quadrant the behavior can be approximated by combination of the maximum hydrostatic stress and an octahedral shear stress criteria

$$D_f^{(+)} = (1-\chi)J_1 + \chi\sqrt{J_2'} = fJ_1 + (1-f)\sqrt{J_2'} \tag{5}$$

- in the tension-compression quadrant the behavior can be approximated by combination of the maximum principal tensile stress and an octahedral shear stress criteria in the form of the Pisarenko-Lebedev limiting state theory [2]

$$D_f^{(-)} = (1-\chi)\sigma_{mp} + \chi\sqrt{J_2'} = f\sigma_{mp} + (1-f)\sqrt{J_2'} \tag{6}$$

where

$$\chi = (1-f), \quad f = (1-\chi) \tag{7}$$

By substituting Eq.(3) into (4) and (5) and writing $\lambda = \sigma_2/\sigma_1$, the stress function can be represented in the normalized form:

- plane stress

$$D_f^{(+)} = \sigma_{mp}\left[(1-\chi)(1+\lambda) + \chi\sqrt{1-\lambda+\lambda^2}\right] \tag{8}$$

$$D_f^{(-)} = \sigma_{mp}\left[(1-\chi) + \chi\sqrt{1-\lambda+\lambda^2}\right] \tag{9}$$

- plane strain

$$D_f^{(+)} = \sigma_{mp}\left[(1-\chi)(1+\lambda)(1+\nu)+\chi\sqrt{1-\lambda+\lambda^2+\nu(1+\nu)\left(1+\lambda^2\right)}\right] \tag{10}$$

$$D_f^{(-)} = \sigma_{mp}\left[(1-\chi)+\chi\sqrt{1-\lambda+\lambda^2+\nu(1+\nu)\left(1+\lambda^2\right)}\right] \tag{11}$$

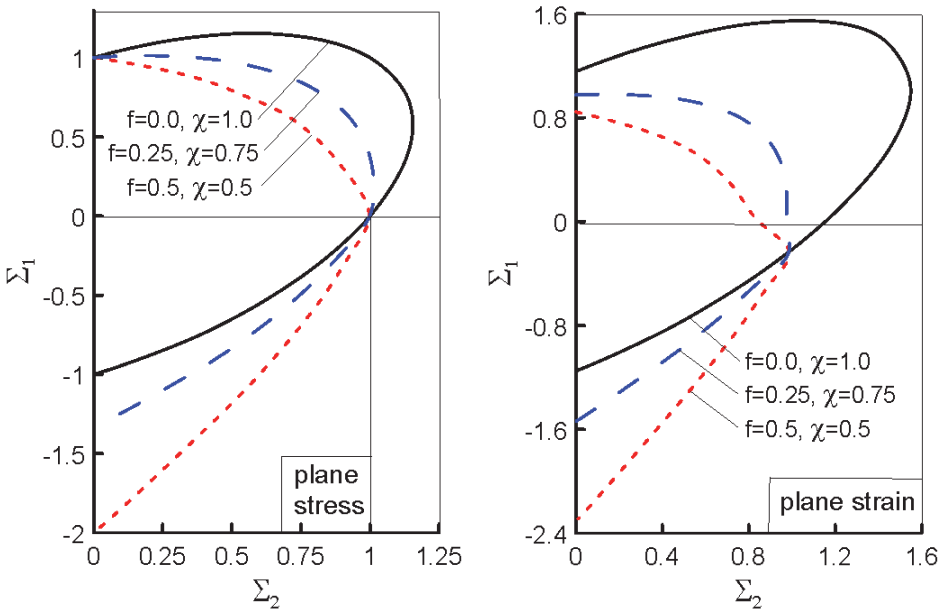


Figure 1: Rupture loci computed from multi-axial stress functions.

By writing $\Sigma_i = \sigma_i/\sigma_0$ where $\sigma_0$ is uniaxial rupture stress, the magnitudes of the biaxial stresses can be determined for different values of the governing material parameter $\chi$. In Fig.1, the results of calculations are shown for plane stress and plane strain conditions using Eqs.(8-11). For constant rupture time the particular forms (8-11) of general relationships (5,6), show a marked sensitivity to stress biaxiality and material constant $\chi$. It would clear therefore that in order to obtain material constants that govern the behavior of general stress function in the form of Eqs.(5,6) two sets of standard tests should be conducted: first set to determine the uniaxial tensile rupture characteristics, a second set carried out under uniaxial compression. The tests carried out under uniaxial compression, as it shown in Fig.1, are the most sensitive in their response to the material behavior under multi-axial stress conditions.

## CREEP DAMAGE FUNCTION

Let $\omega$ denote the measure of damage with $\omega = 0$ denoting the undamaged state and $\omega = 1$ the fully damaged state. An equation describing the evolution of damage under a multi-axial stress state has been proposed by Hayhurst [1]

$$\dot{\omega} = \frac{A\left\{\alpha\sigma_{mp}+\beta J_1+\gamma\sqrt{J_2'}\right\}^{\delta}}{(1+\phi)(1-\omega)^{\phi}} \tag{12}$$

Similarly, we introduce a function for rate of accumulation of creep damage as follows

$$\dot{\omega} = C\left[\frac{D_f^{(\pm)}}{(1-\omega)}\right]^m \tag{13}$$

where $C$ and $m$ are material constants and multi-axial stress function $D_f^{(\pm)}$ described by Eqs.(5,6). By assuming that the creep strain rate is governing by the equivalent von Mises stress, the damage accumulation constitutive equation in multi-axial state of stress is used in the form given by Kachanov [9]

$$\dot{\varepsilon}_{eqv} = B\left(\frac{\sigma_{eqv}}{1-\omega}\right)^n \tag{14}$$

where $B$ and $n$ are constants of the Norton power law equation.

## CREEP STRESS INTENSITY FACTOR

In [10] one unified parameter in the form of a plastic stress intensity factor (SIF) is introduced based on the asymptotic elastic-plastic stress and strain the crack tip fields which gives more accurate the characterization of fracture resistant properties materials and structures under static and cyclic loading than the wide spread two-parametric theories. The plastic SIF takes into account both the in-plane and out-of-plane constraint effects at fracture. Generally, the creep crack-tip singular asymptotic fields in the terms of a creep SIF's under the secondary extensive creep conditions can be modified to obtain a stress, strain and displacement rate for elastic-nonlinear-viscous material properties as the follows [11]

$$\overline{K}_{cr} = \left(\frac{C^*}{\dot{\varepsilon}_0\sigma_0 I_n L}\right)^{1/(n+1)} \quad ; \quad \overline{K}_{\varepsilon,cr} = \overline{K}_{cr}^n \tag{15}$$

For a crack of length $2a$ in an infinite body and subject to a remote stress $\sigma$, $C^*$ for the plane strain problem is given by [4]

$$C^* = \dot{\varepsilon}_0\sigma_0 a\pi\sqrt{n}\left[\frac{\sqrt{3}}{2}\frac{\sigma}{\sigma_0}\right]^{n+1} \tag{16}$$

where $\sigma_0$ and $\dot{\varepsilon}_0$ are reference stress and strain rate, respectively. Equations for the crack tip asymptotic stress-strain fields for three-dimensional creeping solids through amplitude factor (Eq.15) are a function of a governing parameter in the form of creep $I_n$-integral. The numerical method was introduced by the authors [11] to determine the $I_n$-integral for power-law creeping materials. According to this approach, the dimensionless angular stress $\tilde{\sigma}_{ij}^{FEM}$ and displacement rate $\dot{\tilde{u}}_i$ functions are directly determined from the FEA distributions

$$I_n^{FEM}(\theta,t,n) = \int_{-\pi}^{\pi} \Omega^{FEM}(\theta,t,n)\, d\theta \tag{17}$$

$$\begin{aligned}\Omega^{FEM}(\theta,t,n) = {} & \frac{n}{n+1}\left(\tilde{\sigma}_e^{FEM}\right)^{n+1}\cos\theta - \left[\tilde{\sigma}_{rr}^{FEM}\left(\dot{\tilde{u}}_\theta^{FEM} - \frac{d\dot{\tilde{u}}_r^{FEM}}{d\theta}\right) - \tilde{\sigma}_{r\theta}^{FEM}\left(\dot{\tilde{u}}_r^{FEM} + \frac{d\dot{\tilde{u}}_\theta^{FEM}}{d\theta}\right)\right]\sin\theta \\ & - \frac{1}{n+1}\left(\tilde{\sigma}_{rr}^{FEM}\dot{\tilde{u}}_r^{FEM} + \tilde{\sigma}_{r\theta}^{FEM}\dot{\tilde{u}}_\theta^{FEM}\right)\cos\theta\end{aligned} \tag{18}$$

$$\dot{\tilde{u}}_i^{FEM} = \frac{\dot{u}_i^{FEM}}{BL\left(K_{cr}^{FEM}\right)^n}\overline{r}^{\frac{n}{n+1}} = \frac{\dot{u}_i^{FEM}\sigma_0^n}{\dot{\varepsilon}_0 L}\left(\frac{\tilde{\sigma}_e^{FEM}}{\sigma_e^{FEM}}\right)^n = \frac{\dot{u}_i^{FEM}}{\dot{\varepsilon}_0 L}\left(\frac{\tilde{\sigma}_e^{FEM}}{\overline{\sigma}_e^{FEM}}\right)^n = \frac{du_i^{FEM}}{dt}\frac{1}{\dot{\varepsilon}_0 L}\left(\frac{\tilde{\sigma}_e^{FEM}}{\overline{\sigma}_e^{FEM}}\right)^n \tag{19}$$

where $t$ is creep time, $\tilde{\sigma}_e$ is the Mises equivalent stress and $\bar{\sigma}_e^{FEM} = \sigma_e^{FEM} / \sigma_0$. As is usual in mathematical analysis a dot over a displacement quantity denotes a time differentiation. The numerical parameter $I_n$-integral and the $\theta$-variation angular functions of the suitably normalized functions $\tilde{\sigma}_{ij}$ and $\dot{\tilde{u}}_i$ depend on the creep exponent $n$. In the contrary to the traditional models for creep crack growth prediction that the $I_n$-integral is a function only the creep exponent, in the present work it will be demonstrated that this governing parameter depends on the creep damage function and the creeping crack tip stress-strain fields.

## RESULTS AND DISCUSSION

Plane strain finite element analysis was performed based on ANSYS FE-code for study of the creep damage effect on the nonlinear crack tip stress-strain fields for center cracked plate (CCP) subjected to a uniform tensile stress of magnitude $\sigma$=50 MPa. The CCP configuration contains an internal crack of length $2a$=20mm ($a/w$ =0.01, where $w$ is plate width). The 2D plane strain eight-node isoparametric elements were applied to CCP geometry. To consider the details of large deformation and blunting of the crack tip, a typical FE-mesh was used with the initial notch root radius $\rho/a$ =0.01. For creeping undamaged and damaged materials we consider five stages of creep time which is varied from $t$ = 1 hrs up to $t$ = $10^3$ hrs. The creep properties of analyzed material at the elevated temperature of 550°C are summarized in Table 1.

| E [GPa] | ν | B [1/(MPa^n·hr)] | n | C [1/(MPa^m·hr)] |
|---|---|---|---|---|
| 200 | 0.3 | $1\times10^{-14}$ | 5.0 | $1\times10^{-10}$ |

Table 1: The creep properties of material.

Employing the constitutive equations (13,14) directly into the FEM rate-dependent formulation and using an explicit time integration procedure leads to a standard Runge-Kutta integration scheme in which the finite element stiffness matrix is derived from elastic moduli. After the solution of a nonlinear problem, the ANSYS output file is used as an input data for special code developed to determine dimensionless stress-strain angular distributions, damage contour and creep stress intensity factor.

Note that for creeping material, the damage evolution depends generally on the creep time, magnitude of the applied loading, crack geometry and material properties. Due to complexities we consider in the present study different creeping stages. In this case it is useful to normalize a current creep time $t$ by the characteristic time $t_T$ for transition from small-scale creep to extensive creep which is given as [7]

$$\frac{t}{t_T} = \frac{t(n+1)EC}{\left(1-\nu^2\right)K_1^2} \tag{20}$$

where $K_I$ is elastic stress intensity factor, $\nu$ is the Poisson's ratio, $E$ is the Young's modulus and $C$ -integral is given by Eq.(16). In our case the transition time for given nominal stress $\sigma$=50 MPa and crack length $a$ =10mm is $t_T$ = 21.88 hrs. In order to explore the effects of damage formulation, comparisons for $\sigma$ =50 MPa and creep time $t/t_T$ = 45.7 are made in Fig.2 between the HRR-field, undamaged creep field and defective fields at the crack tip in creeping solids. Near the crack tip the influence of the damage degree is evident and the sufficient difference between the HRR and creep damage fields is observed. The data presented in Fig.2 demonstrate the effect of creep damage behaviour on the crack tip fields. Furthermore, it is no longer true that $\theta$-variations of the stresses are independent of creep damage parameter $\omega$.

A fracture damage zone (FDZ) or fracture process zone (FPZ) local to the crack tip is defined as a core where microstructure damage accumulates until crack growth takes place at the macroscopic scale level. Microstructure damages can include void nucleation, growth and coalescence and it is assumed that local fracture will occur at the crack tip when the creep ductility of the material is exhausted there. This process is governed by combination of the maximum principal stress $\sigma_{mp}$ and the stress invariants $J_1$ and $J_2'$. Once these stress invariants have been determined during FEM procedure the creep damage distribution or the FPZ shape and size are obtained by a numerical integration of Eq.(13). In Fig.3

shown contours of damage zones around the crack tip at σ=50Mpa and creep time $t/t_T$ = 45.7 for material different properties defined by the value of constant $\chi=\sigma_t/\sigma_c$. Contours in Fig.4 demonstrated process of the crack tip damage accumulation as a function of creep time.

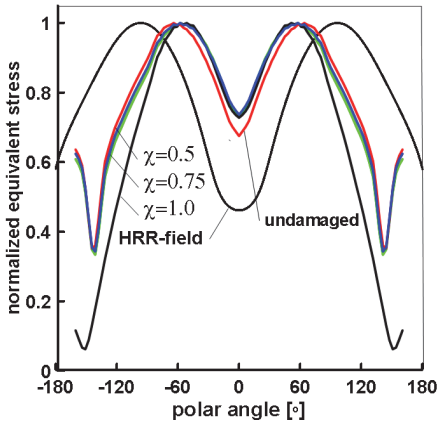


Figure 2: Von Mises equivalent stress angular distributions for different solids states.

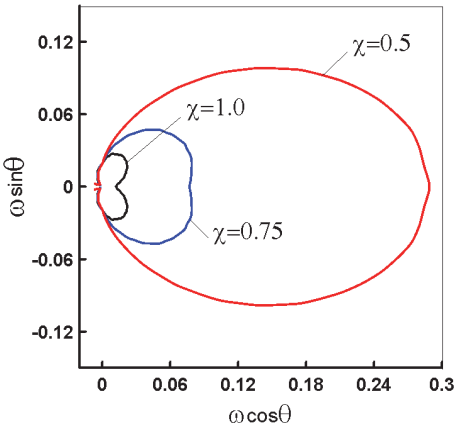


Figure 3: Contours of damage around crack tip at σ=50Mpa and creep time $t/t_T$ =45.7.

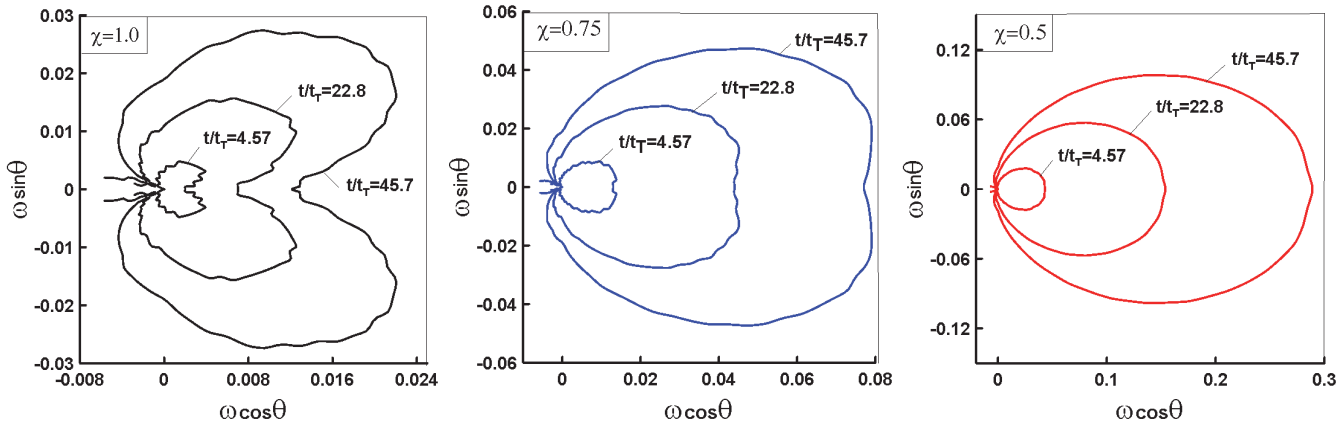


Figure 4: Contours of damage around crack tip as a function of creep holding time.

The important factor in the present study is the influence of state of stress on the damage process. To this end a plane strain analysis of a plate containing an internal crack of relative length $a/w$ =0.01 which is loaded by remote tension was also carried out. In Fig.5 the numerical results for the maximum size of creep damage zone behavior are shown as a function of creep time. It follows from these data, in essence, maximum damage size is sensitive to the maximum principal stress or to the hydrostatic stress through effective stress function formulation by Eqs.(5,6). An increase in hydrostatic stress with $\chi < 1$, then increases the damage zone leading to failure at lower strains and lower times.

As in the case of the dimensionless stress angular distributions $\tilde{\sigma}_{ij}$ (Fig.2), the main effect of damage parameter $\omega$ or material properties $\chi$ on the dimensionless displacement rate components $\dot{\tilde{u}}_i$ arises through the normalizing factor in the form of creep $I_n$ -integral (Eqs.17-19). Figure 6,a represents variation of the $I_n$ -integral distributions through the creep stage for different values of the governing parameter $\chi$ for material behavior constitutive equation. It should be noted that the values for creep $I_n$ -integral do not coincide with those of the HRR elastic-plastic field $I_n^{HRR}$ = 5.024 at the same hardening exponent $n$ = 5. Furthermore, in the frame of creeping solids formulation, $I_n$ -integral distributions as a function of creep time for undamaged and defective materials are different and these distinctions increase with increasing of the holding time. It is obvious that in creeping solids the behavior of the governing parameter of crack-tip field with elapsed time beyond $t/t_T > 1$ is very sensitive to the material constant $\chi = \sigma_t/\sigma_c$ variation.

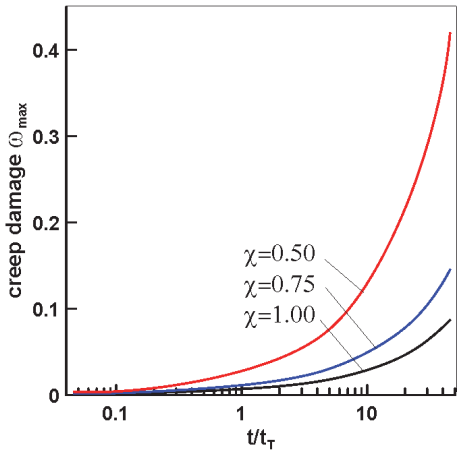


Figure 5: Crack tip damage zone maximum size as a function of creep time.

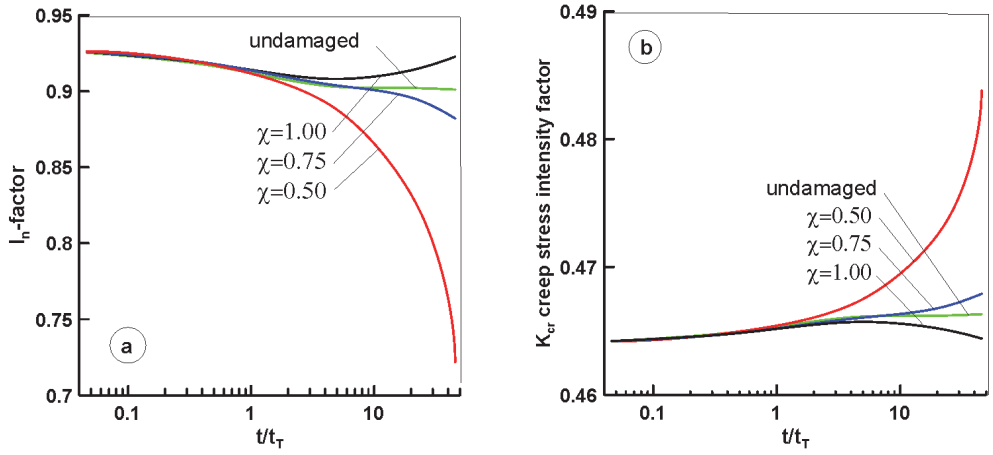


Figure 6: $I_n$-factor (a) and (b) creep stress intensity factor behavior as a function of creep time.

Finally Fig.6,b represents the corresponding numerical results for creep stress intensity factor behavior as a function of creep time according to Eq.(15). The curve concerns to the undamaged material for the steady state of secondary creep solution is also shown in this figure. The creep damage rate dependence of creep stress intensity factor arises from the time dependence of the $I_n$-integral. Again it is clear that the effect of damage evolution appears at the extensive creep condition behind of the small-scale state when the transition time $t/t_T > 1$.

It should be note that as recommended by corresponding ASTM standards, the description of the crack growth rate under creep and creep-fatigue conditions should be given in the terms of $C(t)$ or $C^*$-integral. However, this parameter a-priory may not take into account the effect of the accumulation and growth of damage. Unlike the definition for the elastic stress intensity factor and $C$-parameters, the creep stress intensity factor approach gives the possibility to obtain the crack growth rate as a function of creep damage. To this end, it was necessary to calculate the $I_n$-integral distribution for each crack front position corresponds to a certain combination crack length and creep time and as consequence accumulated creep damage. Recall that in the present study all calculations carried out for the stationary crack under steady state secondary creep conditions. Going back to the crack growth interpretation it should be noted that the effect of the creep damage accumulation on the creep crack growth rate may be scaled through the corresponding value of the creep stress intensity factor. In addition, an inherent property of the creep SIF is their dependence on the multi-axial state of stress through the equation for the damage function (13). Under certain circumstances, this numerical solution may also have application to creeping solids which undergo damaging near the crack tip. Thus, the creep SIF may by identified as damage sensitive high temperature fracture parameter for correlating crack growth under multi-axial stress of state conditions.

## CONCLUSIONS

The effects of material damage on the stress field, shape and size of fracture process zone of a mode I creep crack were investigated on the basis of continuum damage mechanics by using multi-axial stress function. Two cases of continuum solids state, i.e. undamaged creeping material and defective material with different degree of creep damage, were examined. A governing parameter of damage field for creeping solids under multi-axial stress state represented by the experimental constant in the form of ratio uniaxial tensile rupture strength to compression at an appropriate test temperature. It has been shown that the creep holding time and multi-axial states of stress may be combined to produce a method on the basis of creep stress intensity factor for quantifying the damage effects on creep crack growth rate.

## ACKNOWLEDGMENTS

The author gratefully acknowledges the financial support of the Russian Science Foundation under the Project 17-19-01614.

## REFERENCES

[1] Hayhurst, D.R., Creep rupture under multi-axial states of stress, J. Mech. Phys. Solids, 20 (1972) 381–390.
[2] Pisarenko, G. S., Lebedev, A.A., Deformation and Strength of Materials under Complex State of Stress, Naukova Dumka, Kiev, (1976).
[3] Hutchinson, J.W., Constitutive behavior and crack tip fields for materials undergoing creep-constrained grain boundary cavitation, Acta Metall., 31 (1983) 1079–1088.
[4] He, M.Y., Hutchinson, J.W., in: Elastic-Plastic Fracture, v.1, ASTM STP 803, American Society for Testing and Materials, Philadelphia, (1983) 227–290.
[5] Qinghua Meng, Zhenqing Wang, Asymptotic solutions of mode I steady growth crack in materials under creep conditions, Acta Mech. Solida Sinica, 28 (2015) 578–591.
[6] Murakami, S., Hirano, T., Liu, Y., Asymptotic fields of stress and damage of a mode I creep crack in steady-state growth, Int. J. Solids Struct., 37 (2000) 6203–6220.
[7] Li, F.Z, Needleman, A., Shih, C.F., Characterization of near tip stress and deformation fields in creeping solids, Int. J. Fract., 36 (1988) 163–186.
[8] Budden J.P., Ainsworth, R.A., The effect of constraint on creep fracture assessments, Int. J. Fract., 87 (1997) 139–149.
[9] Kachanov, L.M., Introduction to Continuum Damage Mechanics, Martinus-Nijhoff, Dordrecht, (1986).
[10] Shlyannikov, V.N., Tumanov, A.V., Characterization of crack tip stress fields in test specimens using mode mixity parameters, Int. J. Fract., 185 (2014) 49–76.
[11] Shlyannikov, V.N., Tumanov, A.V., Boychenko, N.V., A creep stress intensity factor approach to creep-fatigue crack growth, Engng. Fract. Mech., 142 (2015) 201–219.